KeA1

CHINESE ROOTS
GLOBAL IMPACT

Contents lists available at ScienceDirect

# Petroleum Science

journal homepage: www.keaipublishing.com/en/journals/petroleum-science



Original Paper

# Analysis of sensitivity to hydrate blockage risk in natural gas gathering pipeline



Ao-Yang Zhang <sup>a</sup>, Meng Cai <sup>b</sup>, Na Wei <sup>a, \*</sup>, Hai-Tao Li <sup>a</sup>, Chao Zhang <sup>a</sup>, Jun Pei <sup>a</sup>, Xin-Wei Wang <sup>a</sup>

- <sup>a</sup> State Key Laboratory of Oil and Gas Reservoir Geology and Exploitation, Southwest Petroleum University, Chengdu, 610500, Sichuan, China
- <sup>b</sup> Research Institute of Production Engineering, Daqing Oilfield Co. Ltd., Daqing, 163453, Heilongjiang, China

#### ARTICLE INFO

# Article history: Received 4 September 2023 Received in revised form 13 December 2023 Accepted 18 January 2024 Available online 19 January 2024

Edited by Jie Hao and Meng-Jiao Zhou

Keywords: Natural gas hydrates Gathering pipeline Temperature variation Hydrate formation rate Sensitivity analysis

## ABSTRACT

During the operational process of natural gas gathering and transmission pipelines, the formation of hydrates is highly probable, leading to uncontrolled movement and aggregation of hydrates. The continuous migration and accumulation of hydrates further contribute to the obstruction of natural gas pipelines, resulting in production reduction, shutdowns, and pressure build-ups. Consequently, a cascade of risks is prone to occur. To address this issue, this study focuses on the operational process of natural gas gathering and transmission pipelines, where a comprehensive framework is established. This framework includes theoretical models for pipeline temperature distribution, pipeline pressure distribution, multiphase flow within the pipeline, hydrate blockage, and numerical solution methods. By analyzing the influence of inlet temperature, inlet pressure, and terminal pressure on hydrate formation within the pipeline, the sensitivity patterns of hydrate blockage risks are derived. The research indicates that reducing inlet pressure and terminal pressure could lead to a decreased maximum hydrate formation rate, potentially mitigating pipeline blockage during natural gas transportation. Furthermore, an increase in inlet temperature and terminal pressure, and a decrease in inlet pressure, results in a displacement of the most probable location for hydrate blockage towards the terminal station. However, it is crucial to note that operating under low-pressure conditions significantly elevates energy consumption within the gathering system, contradicting the operational goal of energy efficiency and reduction of energy consumption. Consequently, for high-pressure gathering pipelines, measures such as raising the inlet temperature or employing inhibitors, electrical heat tracing, and thermal insulation should be adopted to prevent hydrate formation during natural gas transportation. Moreover, considering abnormal conditions such as gas well production and pipeline network shutdowns, which could potentially trigger hydrate formation, the installation of methanol injection connectors remains necessary to ensure production safety.

© 2024 The Authors. Publishing services by Elsevier B.V. on behalf of KeAi Communications Co. Ltd. This is an open access article under the CC BY-NC-ND license (http://creativecommons.org/licenses/by-nc-nd/4.0/).

#### 1. Introduction

Compared to traditional energy sources such as coal and oil, natural gas possesses several advantages, including a high combustion heat value, minimal pollution, and low greenhouse gas emissions (Hu et al., 2023; Yang et al., 2023b). With the rapid economic growth driving an increased demand for energy, natural gas has become a vital energy source for both households and

industries (Zhang et al., 2021). Natural gas transportation methods encompass pipeline transmission, liquefied transportation, and high-pressure cylinder packaging, with pipeline transmission being the predominant mode. The safety of natural gas transportation merits our attention. Due to varying fluid properties and complex temperature and pressure fluctuations during the gas transmission process, the formation of natural gas hydrates constitutes a significant threat to the safe operation of gas transmission (Aijaz and Fakhruldin, 2016; Chen et al., 2020; Abbasi and Hashim, 2022). As early as 1934, American scientist first identified that natural gas hydrates could lead to blockages in natural gas pipelines (Hammerschmidt, 1934). The formation of hydrates within

E-mail address: 201131010053@stu.swpu.edu.cn (N. Wei).

<sup>\*</sup> Corresponding author.

pipelines can profoundly impact the gas transmission process. Even a small amount of hydrate formation can narrow the gas flow path, induce throttling, increase pressure differentials within the pipeline, thereby accelerating hydrate formation (Tang et al., 2020; Luo et al., 2022). The accumulation of substantial hydrates can result in blockages in pipeline valves and equipment, causing severe damage, and potentially leading to serious pipeline accidents and human casualties (Sun et al., 2021; Wang et al., 2022). Hence, the prevention and mitigation of hydrates in gas pipelines are especially crucial. Natural gas hydrates, also known as "flammable ice", are cage-like crystalline compounds formed by the interaction of natural gas and water under low-temperature, high-pressure conditions (Parsons, 2023; Misyura, 2022). During the natural gas transportation process, the formation of hydrates can readily lead to pipeline blockages, resulting in reduced production, shutdowns, and pressure buildups. Consequently, there is an urgent need to conduct research on the risk-sensitive patterns of hydrate blockages in gas transportation pipelines based on coupled temperature and pressure calculations.

Currently, researchers have extensively investigated the computation of gas pipelines. Freer et al. obtained kinetic parameters for methane hydrate formation through measurements, revealing a proportional relationship between hydrate growth rate and supercooling (Freer et al., 2001); Yang et al. discovered that the unique environment of subsea natural gas reservoirs can also affect the kinetics of hydrate formation(Yang et al., 2023a); Bergeron et al., based on semi-batch stirred reactor experiments, proposed alternative formulas for hydrate growth models(Bergeron and Servio, 2009): Sonne and Pedersen simulated condensate gas transportation pipelines and proposed that key factors for pipeline hydrate formation include hydrate content, liquid holdup, and liquid shear rate (Sonne and Pedersen, 2009); Kishimoto et al. observed hydrate crystal growth and measured lateral hydrate film growth rate (Kishimoto et al., 2011); Webb's experiments discovered a rapid increase in viscosity during slurry hydrate formation(Webb et al., 2012); Rao et al. studied the formation and deposition process of hydrates on pipeline walls in a saturated aqueous methane system(Rao et al., 2013); Joshi et al. proposed a mechanism for gas hydrate blockage in a pure water system (Joshi et al., 2013); Kvamme et al. analyzed the mechanism of hydrate formation in natural gas transportation pipelines containing water and impurities (Kvamme et al., 2016); Akhfash et al. observed the formation, movement, growth, and deposition of hydrate particles in a sapphire high-pressure vessel (Akhfash et al., 2016); Liu et al. established a predictive model for hydrate plugging in deepwater gas wells during testing and analyzed the sensitivity of key factors affecting hydrate plugging(Liu et al., 2018a). These studies have laid the foundation for conducting sensitivity analysis on the risk of hydrate blockage in natural gas transportation pipelines.

Therefore, based on the previously summarized equilibrium models of hydrates, a comprehensive theoretical framework has been developed for the operation of natural gas gathering pipelines. This framework encompasses the theory of pipeline temperature distribution, pipeline pressure distribution, multiphase flow, hydrate blockage, and numerical solution methods. The reliability of the predictive methods was validated using data from referenced gathering pipelines, and further research was conducted into the effects of different inlet temperatures, inlet pressures, and terminal pressures on hydrate formation within the gathering pipelines. This analysis revealed the patterns of hydrate blockage under varying conditions, as shown in Fig. 1, it is the Natural gas gathering pipeline (Liu et al., 2018b). Solve complex multiphase flow problems by using a coupled model, and solve problems where it is difficult to obtain hydrate related parameters (hydrate formation rate, blockage location, etc.). This provides a

new perspective and method for the prevention and control of gas hydrates in natural gas gathering and transportation.

# 2. Hydrate blockage prediction model

The distribution of temperature and pressure within gathering pipelines, along with the equilibrium conditions of natural gas hydrates, constitutes a key factor for predicting the risk of hydrate formation. These equilibrium conditions are primarily influenced by fluid composition, inhibitor type, and content. By incorporating calculations of pipeline temperature, pressure, and hydrate equilibrium conditions, a predictive method for hydrate formation within gathering pipelines was established. During the natural gas transmission process, a comparison between the internal pipeline temperature, pressure, and hydrate equilibrium conditions reveals that if the temperature at a certain point in the pipeline falls below the hydrate equilibrium temperature and the pressure exceeds the hydrate equilibrium pressure in the presence of water, it indicates that the conditions for hydrate formation are met at that point. This signifies the existence of a hydrate formation risk within the pipeline (Wang et al., 2014). The difference between the fluid temperature within the pipeline and the hydrate equilibrium temperature is referred to as the hydrate formation supercooling degree. The higher the supercooling degree under conditions conducive to hydrate formation, the greater the risk of hydrate

To facilitate the study and considering practical scenarios, the following assumptions are made for the hydrate blockage assessment model within gathering pipelines:

- (1) Assuming steady one-dimensional flow of compressible fluid within the pipeline.
- (2) The rate of hydrate formation on the pipeline wall's liquid film is approximately equal to the rate of hydrate formation on the liquid film.
- (3) Given the nature of natural gas long-distance pipelines, the hydrate induction period is very short, and ice formation is neglected when the flow temperature approaches the freezing point of water.
- (4) During a relatively long stable period, external environmental temperature parameters remain constant.

# 2.1. Multiphase flow model

At a distance of x from the starting point, select a fluid with a



Fig. 1. Natural gas gathering pipeline.

length of dz as control body, as shown in Fig. 2.

Hence, the multiphase flow equation for gathering pipelines is given by

$$\begin{split} &\frac{\partial}{\partial t} \left( \rho_{g} \alpha_{g} \nu_{g} + \rho_{l} \alpha_{l} \nu_{l} + \rho_{s} \alpha_{s} \nu_{s} \right) + \frac{\partial}{\partial z} \left( P_{x} + \rho_{g} \alpha_{g} \nu_{g}^{2} + \rho_{l} \alpha_{l} \nu_{l}^{2} + \rho_{s} \alpha_{s} \nu_{s}^{2} \right) \\ &+ \left( \rho_{g} \alpha_{g} + \rho_{l} \alpha_{l} + \rho_{s} \alpha_{s} \right) g \sin \theta = 0 \end{split} \tag{1}$$

where, according to the theory of continuous medium, we have

$$\alpha_{\mathbf{g}} + \alpha_{\mathbf{l}} + \alpha_{\mathbf{s}} = 1 \tag{2}$$

In the equation above,  $\rho_{\rm g}$ ,  $\rho_{\rm l}$ , and  $\rho_{\rm s}$  respectively represent the densities of the gas phase medium, liquid phase medium, and solid phase medium, measured in kg/m³;  $\alpha_{\rm g}$ ,  $\alpha_{\rm l}$ , and  $\alpha_{\rm s}$  denote the holdup of the gas phase medium, liquid phase medium, and solid phase medium within the pipeline, expressed as percentages and dimensionless;  $v_{\rm g}$ ,  $v_{\rm l}$ , and  $v_{\rm s}$  represent the velocities of the gas phase medium, liquid phase medium, and solid phase medium within the pipeline, measured in m/s;  $P_x$  signifies the pressure at any point within the gathering pipeline, measured in Pa; g represents the acceleration due to gravity, measured in m/s²; and  $\theta$  indicates the inclination angle of the pipeline, measured in degrees, with  $\theta=0^\circ$  for a horizontal pipeline.

#### 2.2. Pipeline temperature distribution model

Based on the principles of the law of energy conservation and the fundamental heat conduction equation (Cai et al., 2018; Bykov et al., 2022), a model for the distribution of temperature in the pipeline has been developed. At a distance *x* from the starting point, an infinitesimal section of the pipe is selected. Within a unit of time, the heat lost from the medium within this pipe segment to the surrounding soil is equal to the heat released by the medium, as follows:

$$-Mc_{p}dT = K\pi Ddx(T - T_{a})$$
(3)

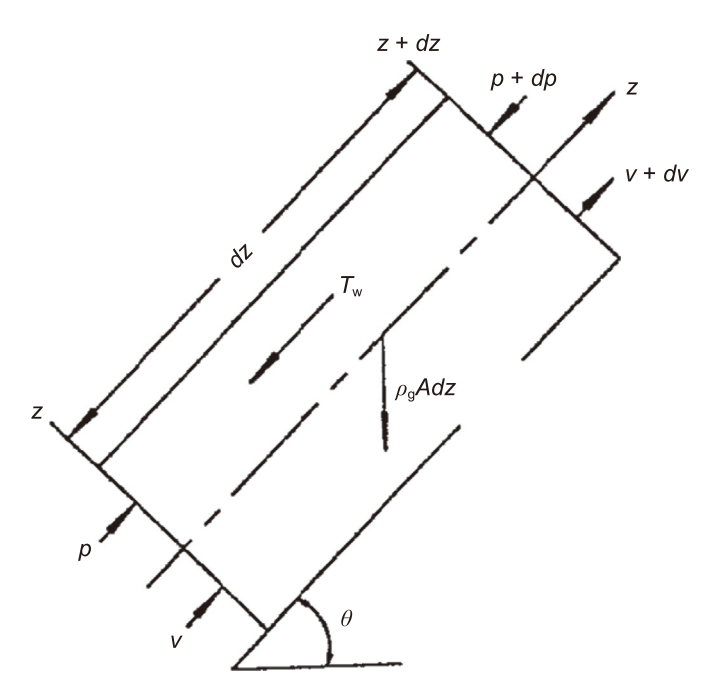


Fig. 2. Control volume.

After separating the variables and performing integration, we have

$$\int_{T_0}^{T_x} \frac{dT}{T - T_a} = -\int_0^x \frac{K\pi D}{Mc_p} dx$$
 (4)

The solution is obtained as follows:

$$T_x = T_a + (T_0 - T_a)e^{-ax}$$
 (5)

wherein, we have

$$a = \frac{K\pi D}{Mc_{\rm p}} \tag{6}$$

In the equation: M represents the mass flow rate of the medium, measured in kg/s;  $c_p$  represents the specific heat capacity of the medium, expressed in J/(kg·K); dT stands for the temperature change, indicated in K; K denotes the heat transfer coefficient, given in W/( $m^2$ ·K); D signifies the pipe diameter, measured in meters; x represents the distance from the starting point to this specific location, in meters;  $T_x$ ,  $T_0$ , and  $T_a$  respectively indicate the temperature of the medium at a distance x from the starting point, the temperature at the starting point, and the ambient soil temperature, all measured in K.

#### 2.3. Pipeline pressure distribution model

The pipeline pressure distribution model is established for natural gas gathering and transportation processes (Jiang et al., 2022). Assuming the flow within the pipeline is steady-state, one-dimensional, compressible fluid flow, the pressure distribution is calculated using the Weymouth's formula, as follows:

$$P_{x} = \left[ P_{1}^{2} - \left( P_{1}^{2} - P_{2}^{2} \right) \frac{x_{1}}{l} \right]^{0.5} \tag{7}$$

In the initial segment of the gas pipeline, the pressure gradually decreases along the length of the pipe, and as it approaches the end, the pressure drop becomes more rapid. Therefore, within the gas pipeline, the pressure does not change linearly. In the equation,  $P_1$  and  $P_2$  represent the starting pressure and ending pressure, respectively, in Pa, and I represents the total length of the gathering pipeline in meters.

#### 2.4. Hydrate blockage model

From a dynamic perspective, the formation of hydrates involves two processes: nucleation and growth. Nucleation marks the onset of phase transition, where micro-sized hydrate crystals attempt to reach critical dimensions. This is a stochastic micro-scale process, imperceptible at the macroscopic level. Due to hydrate formation, the solid phase content within the flowing system increases, leading to heightened viscosity and flow resistance. Aggregation among hydrate particles results in the formation of larger hydrate agglomerates, further amplifying flow resistance and ultimately leading to blockage. Refer to Fig. 3.

Subcooling refers to the difference between the equilibrium temperature for hydrate formation at a given pressure and the actual temperature. Induction time refers to the duration between contact initiation of host and guest molecules to the formation of hydrate nuclei. The induction time for natural gas hydrate formation in a flowing system is influenced by pressure and liquid flow velocity. Hydrate nucleation and growth processes occur simultaneously, and subcooling can be expressed as

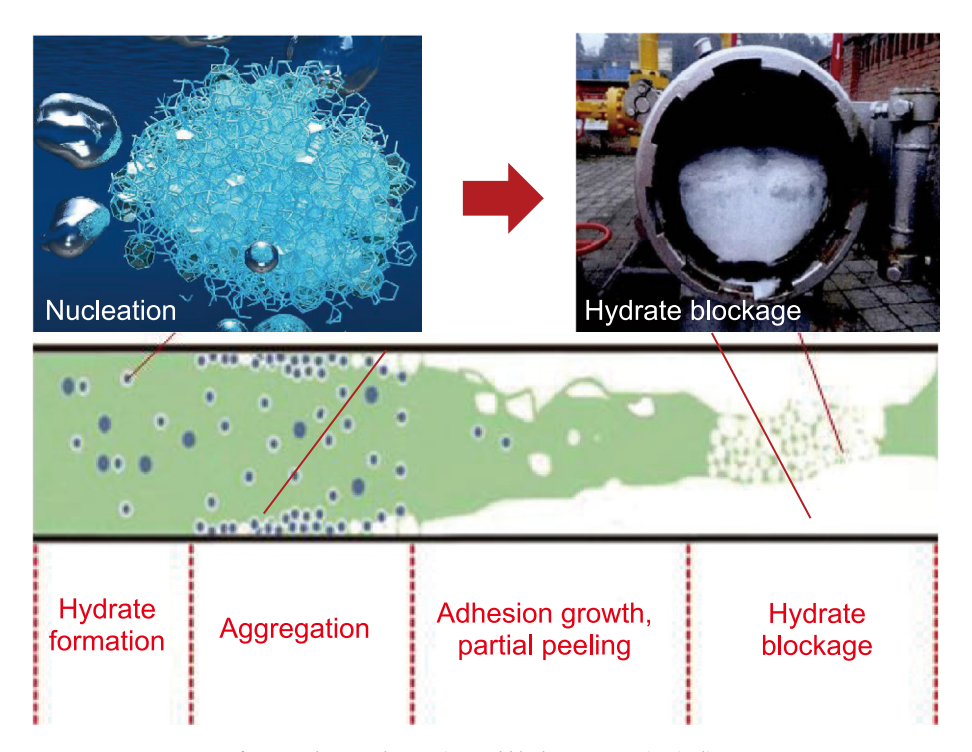


Fig. 3. Hydrate agglomeration and blockage process in pipelines.

$$\Delta T_{\rm sub} = T_{\rm eq} - T_{\rm x} \tag{8}$$

In the natural gas gathering process, the deposition of hydrate particles generated from liquid droplets onto pipe walls cannot be ignored. Due to the presence of free water on the pipe wall, the adhesion force between hydrate particles and the wall is greater than that between hydrate particles. Research indicates that higher flow velocities can also enhance gas disturbance, thereby inhibiting hydrate formation and aggregation. The rate of hydrate formation on the pipe wall liquid film is approximately equal to the rate of hydrate formation on the liquid film. The rate of hydrate particle deposition per unit length of pipeline is given by (Ren et al., 2019):

$$R_{\rm hd} = \frac{2\pi r_{\rm f} u k_1 M_{\rm h}}{M_{\rm g}} \exp\left(-\frac{k_2}{T_x}\right) (\Delta T_{\rm sub}) \tag{9}$$

where

$$T_{\rm eq} = 10.088 \ln P_{\rm x} + 263.4832 \tag{10}$$

Hydrate formation only occurs when equilibrium conditions are met. During the process of hydrate deposition and continuous growth on the pipe wall, the rate of pipe diameter reduction is given by

$$-\frac{\mathrm{d}r_{\mathrm{f}}}{\mathrm{d}t} = \frac{R_{\mathrm{hd}}}{2\pi r_{\mathrm{f}}\rho_{\mathrm{h}}} \tag{11}$$

The thickness of the hydrate film is

$$\delta_{\rm h} = \int_0^t \frac{u k_1 M_{\rm h} \Delta T_{\rm sub}}{\rho_{\rm h} M_{\rm g}} \mathrm{e}^{-k_2/T_{\rm f}} \mathrm{d}t \tag{12}$$

In the equation,  $\Delta T_{\rm sub}$  and  $T_{\rm eq}$  respectively represent subcooling and equilibrium temperature, in K;  $R_{\rm hd}$  represents the rate of hydrate formation in submarine natural gas pipelines, in mol/s;  $r_{\rm f}$  represents the effective diameter, in m;  $k_{\rm 1}$  represents the kinetic

constant, dimensionless;  $k_2$  represents the activation temperature for hydrate formation, in K; u represents the empirical coefficient, dimensionless; and  $\rho_h$  represents the density of hydrates, in kg/m<sup>3</sup>.

#### 3. Model solving and validation

# 3.1. Model solving

In the preceding section, the model and equations for predicting hydrate blockage were presented, some of which are nonlinear. Parameters such as multiphase flow, temperature, pressure, hydrate formation, and deposition rates in the pipeline are interrelated and mutually influential. The pipeline can be discretized into a finite number of nodes along its length. By simultaneously solving the multiphase flow model, pipeline temperature distribution model, pipeline pressure distribution model, and hydrate blockage model, a coupled mathematical model is established and solved using an iterative approach. This process identifies the region of hydrate formation, enabling further investigation into the sensitivity of relevant parameters. The node division and solving process are illustrated in Fig. 4.

Additionally, based on actual conditions, the initial conditions for the aforementioned model solving can be determined as follows:

$$P_{\mathcal{X}}(l) = P_2 \tag{14}$$

The boundary conditions are

$$P_{\mathsf{X}}(0) = P_1 \tag{15}$$

$$T_{\mathsf{x}}(0) = T_{\mathsf{1}} \tag{16}$$

In Fig. 4,  $P_X(l)$  represents the terminal pressure at point l, in Pa; wherein  $P_X(0)$  denotes the starting pressure of the gathering pipeline, in Pa; and  $T_X(0)$  represents the starting pressure of the gathering pipeline, in K. The calculation sequence proceeds from

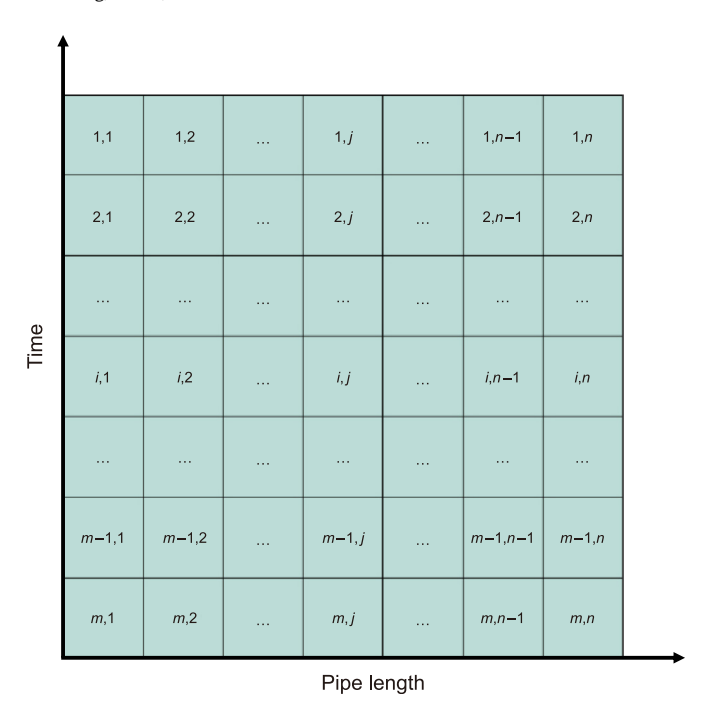


Fig. 4. Grid division of gathering pipeline.

the starting point to the terminal point. Assuming that the parameters at node i within the pipeline are known conditions, the calculation process from node i to (i+1) is illustrated in Fig. 5, where  $\zeta$  signifies the acceptable calculation error.

# 3.2. Model validation

Prior to conducting sensitivity analysis in this study, the proposed theoretical assessment model and numerical simulation calculations are validated by first performing computations and comparisons using data from a terrestrial pipeline referenced in this paper (Liu et al., 2018b). The pipeline has a length of 120 km, an internal diameter of 0.7 m, a relative density of natural gas of 0.632, with methane accounting for 85% composition, an initial pressure of 3.5 MPa, and an initial temperature of 313.15 K. In the validation of the model, the calculated daily gas production for this case is  $180 \times 10^4$  m³, and the daily water production is 2.72 m³. An ambient temperature of 263.15 K is considered, and a coupled analysis of temperature and pressure fields within the gathering pipeline, accounting for the effects of hydrate formation, is performed for this terrestrial pipeline data. The results of the model validation calculations are illustrated in Fig. 6:

For this terrestrial pipeline, a coupled analysis of temperature and pressure fields was conducted to determine the equilibrium temperature for hydrate formation, subsequently identifying the region where hydrate formation occurs. The calculated terminal temperature was 267.85 K, while the actual temperature stood at 264.02 K, resulting in a computation error of 1.45%. The hydrate formation zone was determined to be between 71.72 km and 120.00 km, with the observed formation zone spanning from 68.91 to 120.00 km, leading to a calculation discrepancy of 4.07%. With errors remaining below 5%, they fall within acceptable engineering tolerances. The point of intersection between pipeline temperature and hydrate equilibrium temperature designates the critical point of hydrate formation. Evidently, this pipeline does exhibit hydrate formation, aligning with practical gas well gathering phenomena. The validation of the theoretical model and numerical simulation

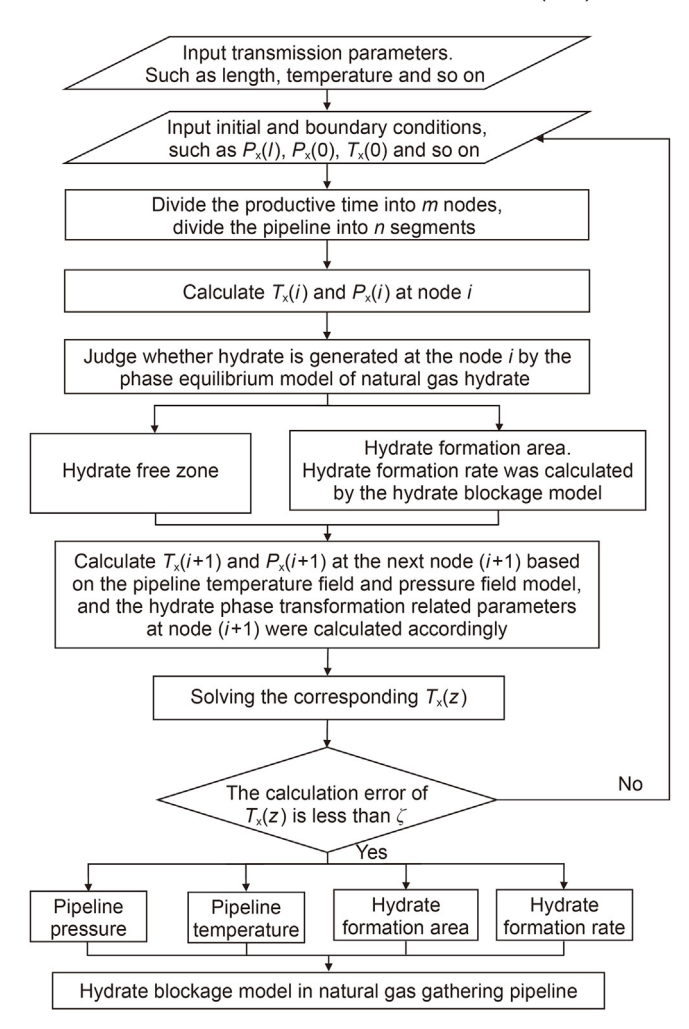


Fig. 5. Calculation flowchart for solving the hydrate blockage model in gathering pipelines.

underscores their accuracy, affirming the high precision of the hydrate formation model and calculation methodology proposed in this paper for natural gas gathering pipelines.

### 4. Results and discussion

For the gas field gathering and transportation process, due to the variable flow conditions within the pipelines and the complex multiphase flow conditions involving certain hydrate-related parameters that cannot be obtained through experiments, the developed solution based on the coupling of temperature and pressure field calculations in the natural gas hydrate plugging model effectively addresses this issue. By utilizing numerical computation methods to solve the plugging assessment model and leveraging data from a specific onshore gas field gathering and transportation operation, multiphase pipeline flow numerical simulations were conducted to calculate hydrate formation plugging parameters for multiphase flow within the pipelines, followed by a sensitivity analysis. Table 1 provides the fundamental domestic natural gas transmission parameters and relevant calculation parameters used in the computation.

The length of the gathering and transportation pipeline is 10 km, with an inner diameter of 700 mm. The average daily gas transmission volume is  $0.527 \times 10^4$  m³/d, and the average daily water transmission volume is 2.725 m³/d. Building upon the

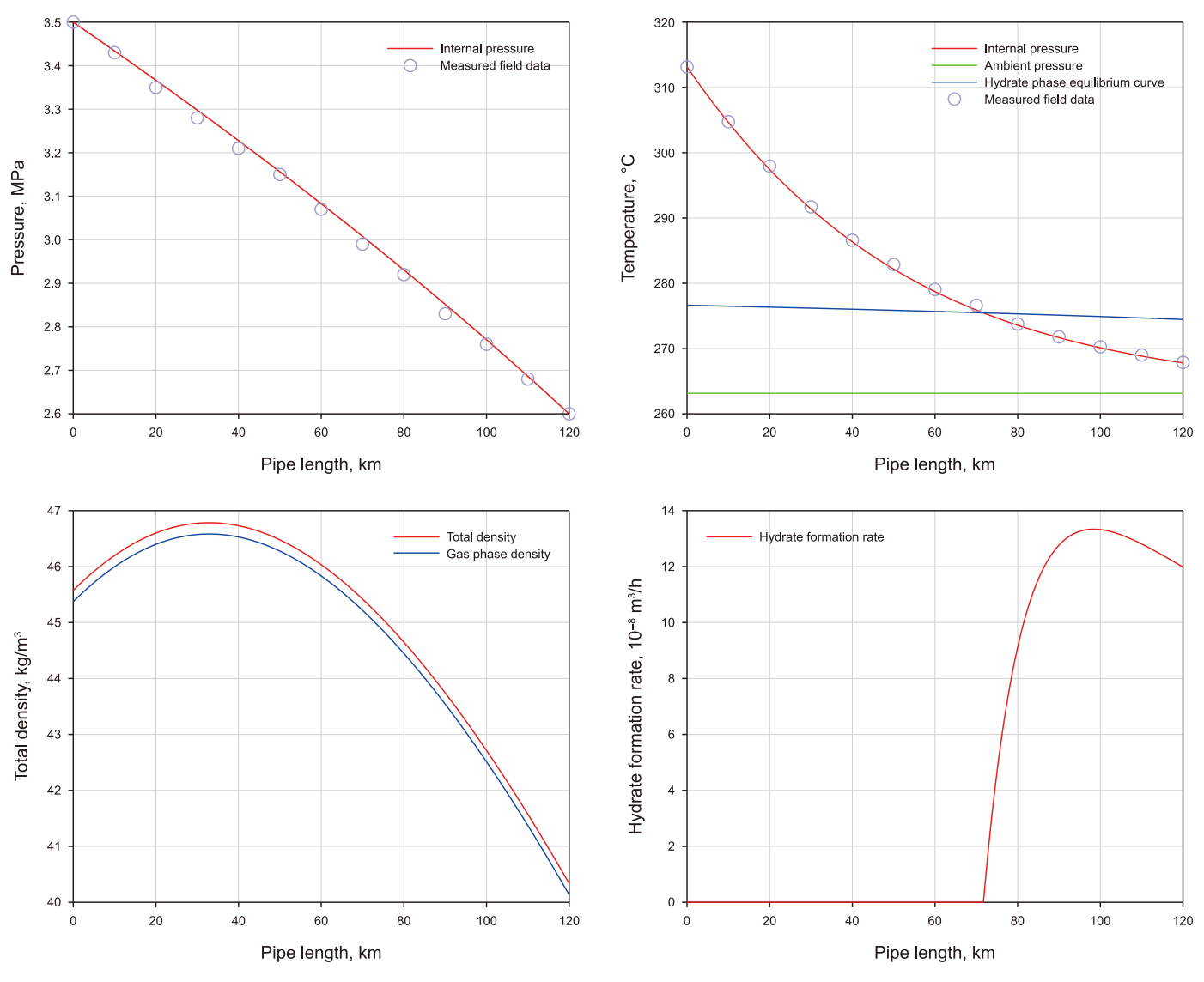


Fig. 6. Model validation outcomes.

**Table 1**Basic transmission and calculation parameters.

Related parameters	Value	Related parameters	Value
Pipeline length, km	10	Pipeline inclination, rad	0
Pipe inner diameter, m	0.70	Water density, kg⋅m <sup>-3</sup>	1010
Average gas transmission rate, 10 <sup>4</sup> m <sup>3</sup> /d	0.527	Viscosity of water, Pa·s	$1.01 \times 10^{-6}$
Average water transmission rate, m <sup>3</sup> /d	2.725	Hydrate density, kg⋅m <sup>-3</sup>	980
Inlet pressure, MPa	5.26	Relative molecular weight of hydrates	176.21
Inlet temperature, K	280.15	Natural gas relative density	0.709
Ambient temperature, K	263.15	Kinetic constant	$2.608 \times 10^{16}$
Water cut	0.05%	Activation temperature for hydrate formation, K	13600
Gas cut	99.95%	Empirical coefficient	0.5

aforementioned natural gas hydrate plugging model within the gathering and transportation pipeline, an analysis is conducted to assess the impact of different inlet temperatures, inlet pressures, and terminal pressures on the system dynamics (Amr et al., 2023; Soroush and Abdollah, 2023; Liu et al., 2023). The sensitivity analysis results are presented in Table 2, showcasing the varying influences.

# 4.1. Effect of inlet temperature

During the operation of the natural gas gathering and transportation pipeline, under conditions of initial flow temperatures of 273.15, 280.15, and 287.15 K respectively, different temperature and pressure distributions within the pipeline were obtained through calculations for various inlet temperatures, as illustrated in Fig. 7.

**Table 2** Sensitivity analysis table.

Number	Inlet temperature, K	Inlet pressure, MPa	Terminal pressure, MPa
1	273.15	5.26	4.88
2	280.15		
3	287.15		
4	280.15	5.06	
5		5.26	
6		5.46	
7		5.26	3.88
8			4.88
9			5.88

From Fig. 7, it can be observed that as the inlet temperature increases from 273.15 to 287.15 K, the temperature at the terminal station increases from 263.83 to 264.82 K. The total density decreases along the pipeline from the starting station to the terminal station, with the rate of decrease diminishing progressively. The

primary reasons for this are as follows: With an increase in inlet temperature, the heat carried by the fluid within the gathering and transportation pipeline increases, leading to an overall rise in temperature along the pipeline. However, due to heat dissipation effects, the flow temperature gradually decreases. If the pipeline were infinitely extended, the flow temperature would tend towards the ambient temperature, i.e., 263.15 K. The trend in flow temperature change predominantly determines the variation trend of total density.

In Fig. 7, when the inlet temperature is 273.15 K, hydrates are generated throughout the entire pipeline section. When the inlet temperature is 280.15 K, the range of hydrate formation narrows to 0.05–10.00 km, and with an inlet temperature of 287.15 K, the range further narrows to 1.38–10.00 km. As the inlet temperature increases from 273.15 to 287.15 K, the maximum hydrate formation rate initially increases and then decreases, rising from  $33.01\times 10^{-8}~\text{m}^3/\text{h}$  to  $33.22\times 10^{-8}~\text{m}^3/\text{h}$  before decreasing to  $32.74\times 10^{-8}~\text{m}^3/\text{h}$ . The most likely location for hydrate plugging

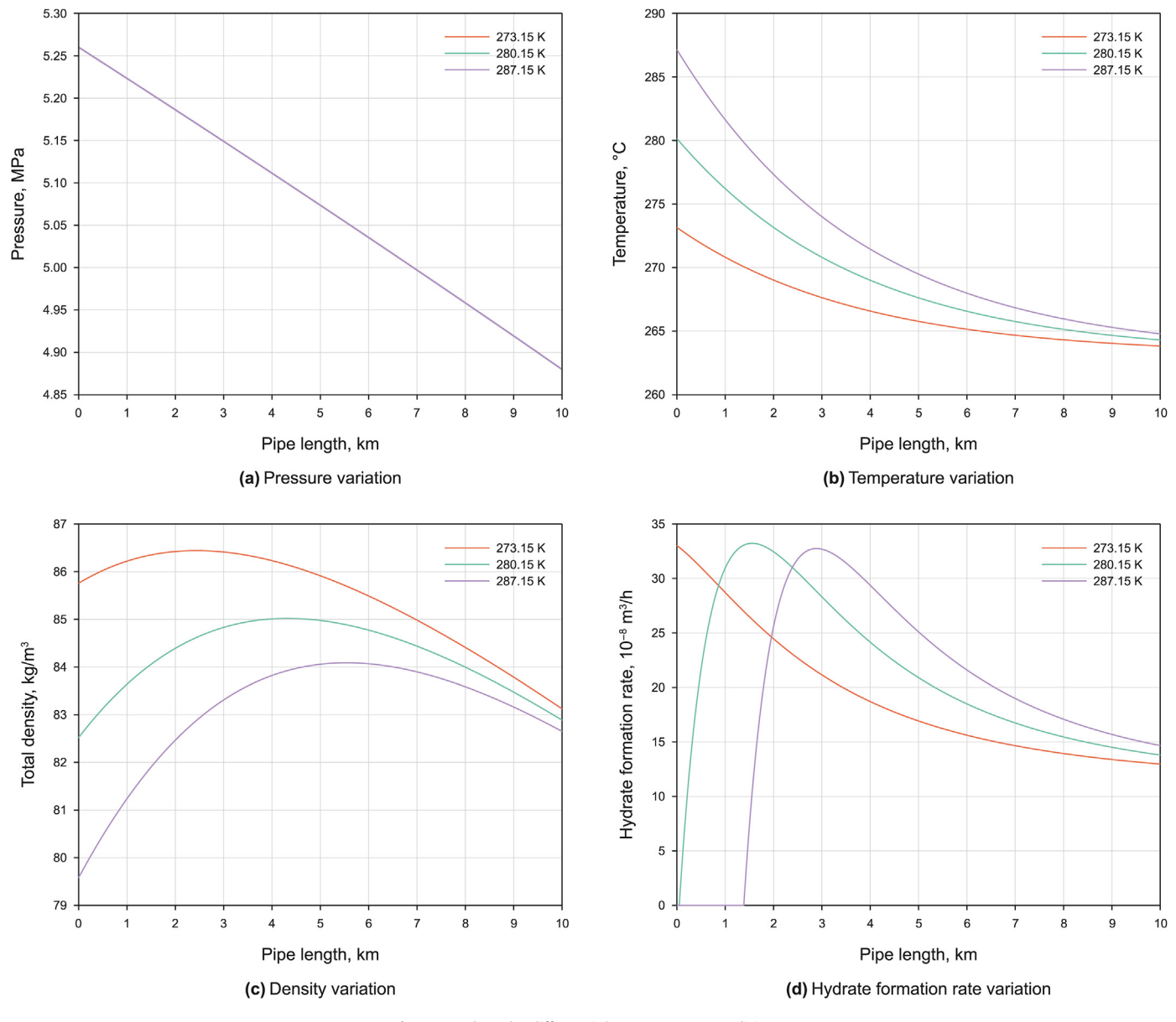


Fig. 7. Trends under different inlet temperature conditions.

shifts from 0 to 1.57 km and then further to 2.88 km. Summarizing the above analysis, in the course of the operation of the natural gas gathering and transportation pipeline, higher inlet temperatures will narrow the range of hydrate formation, reduce hydrate supercooling after formation, and shift the most probable hydrate-plugging location towards the terminal. Higher flow temperatures contribute to ensuring the safety of hydrate prevention and control during the transportation process.

#### 4.2. Effect of inlet pressure

During the operational phase of the natural gas gathering and transportation pipeline, different temperature and pressure distributions within the pipeline under conditions of inlet pressures of 5.06, 5.26, and 5.46 MPa were computed and are presented in Fig. 8.

From Fig. 8, it can be observed that as the inlet pressure increases from 5.06 to 5.46 MPa, the total density increases along the pipeline from the starting station to the terminal station. The rate of

increase, however, diminishes progressively from the starting station to the terminal station. The primary reasons for this are as follows: the trend in flow pressure change predominantly determines the variation trend of total density. When the flow temperature and flow pressure are the same, the total density is also the same, as evident at the gathering terminal station indicated at a pipe length of 10 km.

In Fig. 8, when the inlet pressure is 5.46 MPa, hydrates are generated throughout the entire pipeline section. When the inlet pressure is 5.26 MPa, the range of hydrate formation narrows to 0.05–10.00 km, and with an inlet pressure of 5.06 MPa, the range further narrows to 0.13–10.00 km. As the inlet pressure decreases from 5.46 to 5.06 MPa, the maximum hydrate formation rate continuously decreases from 34.96  $\times$  10<sup>-8</sup> to 31.57  $\times$  10<sup>-8</sup> m³/h. The most likely location for hydrate plugging, after formation, shifts from 1.45 to 1.67 km. Summarizing the above analysis, in the course of the operation of the natural gas gathering and transportation pipeline, lower inlet pressures will lead to a reduction in the

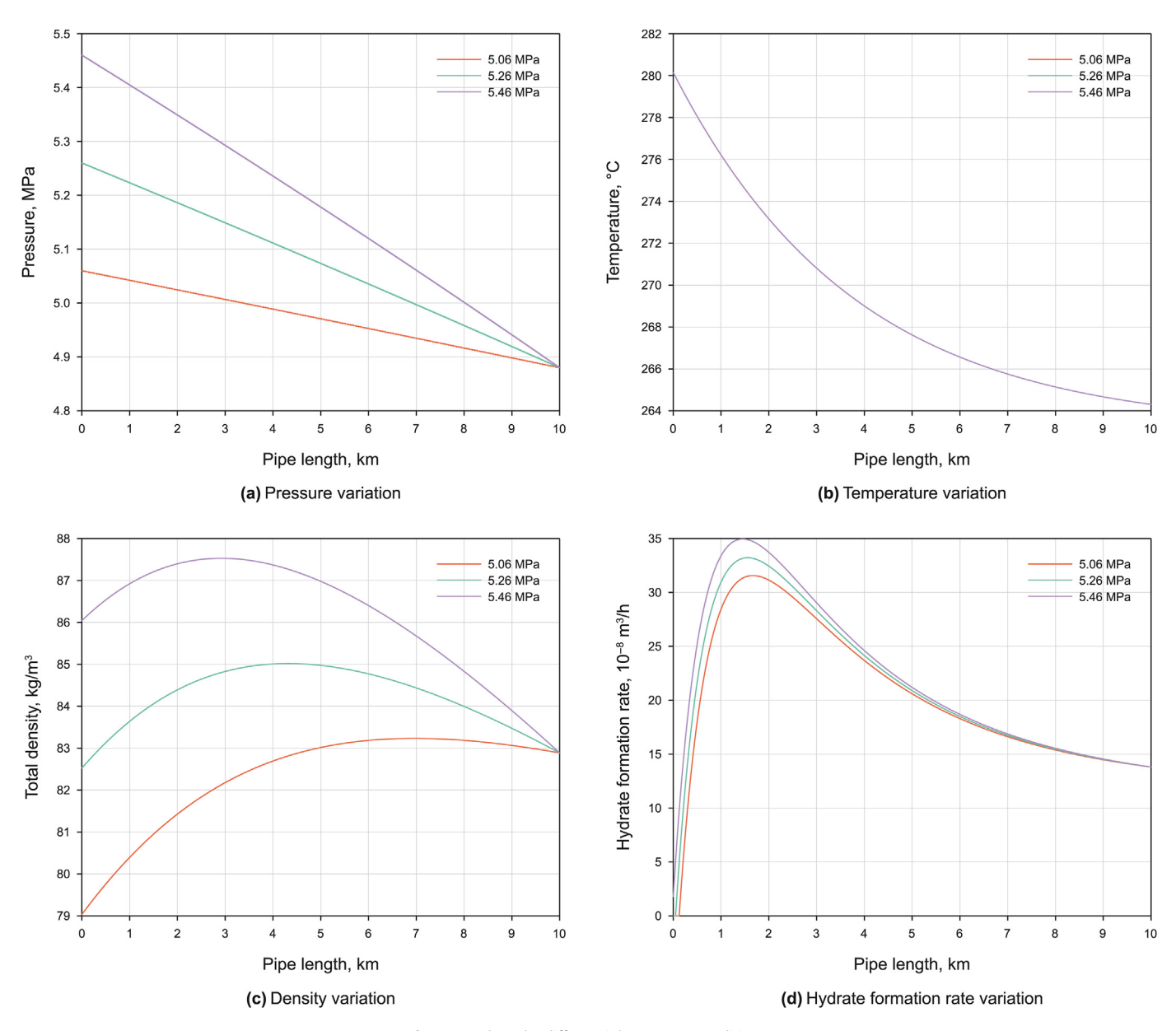


Fig. 8. Trends under different inlet pressure conditions.

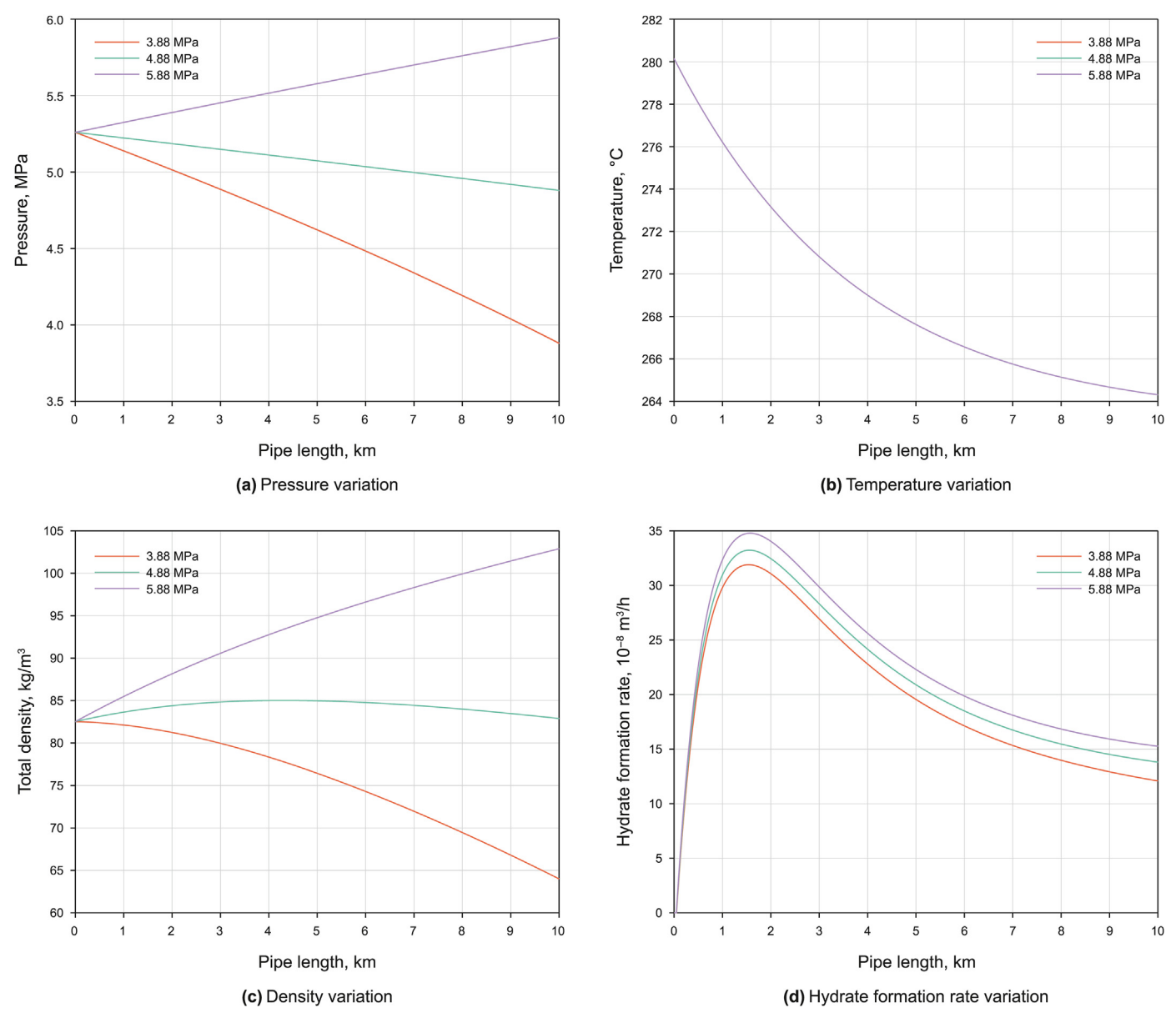


Fig. 9. Trends under different terminal pressure conditions.

maximum hydrate formation rate, a narrowing of the hydrate formation range, and a shift in the most probable hydrate-plugging location towards the terminal. Lower flow pressures contribute to ensuring the safety of hydrate prevention and control during the transportation process.

# 4.3. Effect of terminal pressure

During the operation of the natural gas gathering and transportation pipeline, different temperature and pressure distributions within the pipeline were computed under conditions of

**Table 3**Analysis of hydrate blockage risk in natural gas gathering process under different influencing factors.

Groups	Influencing factors		Maximum hydrate formation rate, $10^{-8} \ m^3/h$	The most likely location for hydrate blockage, km
1	Inlet temperature	273.15 K	33.01	0
2		280.15 K	33.22	1.57
3		287.15 K	32.74	2.88
4	Inlet pressure	5.06 MPa	31.57	1.67
5		5.26 MPa	33.22	1.57
6		5.46 MPa	34.96	1.45
7	Terminal pressure	3.88 MPa	31.89	1.54
8		4.88 MPa	33.22	1.57
9		5.88 MPa	34.78	1.58

From Fig. 9, it is evident that as the terminal pressure increases from 3.88 to 5.88 MPa, the total density increases along the pipeline from the starting station to the terminal station, and the rate of increase progressively rises from the starting station to the terminal

terminal pressures of 3.88, 4.88, and 5.88 MPa, as depicted in Fig. 9.

increase progressively rises from the starting station to the terminal station. The primary reasons for this are as follows: the trend in flow pressure change predominantly determines the variation trend of total density. When the flow temperature and flow pressure are the same, the total density is also the same, as evident at the gathering starting station indicated at a pipe length of 0 km.

In Fig. 9, when the terminal pressure is 3.88, 4.88, or 5.88 MPa, the range of hydrate formation extends from 0.05 to 10.00 km. As the terminal pressure decreases from 5.88 to 3.88 MPa, the maximum hydrate formation rate continuously decreases from  $34.78\times10^{-8}$  to  $31.89\times10^{-8}$  m $^3/h$ . The most likely location for hydrate plugging, after formation, shifts from 1.58 to 1.54 km. Summarizing the above analysis, higher terminal pressure contributes to an increase in the overall density of natural gas, reduces the hydrate formation range, decreases the rate of hydrate formation, and shifts the most likely blockage location towards the terminal station. Conversely, lower terminal pressure would have the opposite effects.

### 4.4. Risk analysis of different influencing factors

Based on the temperature and pressure variations under different conditions of inlet temperature, inlet pressure, and terminal pressure, combined with the hydrate phase equilibrium conditions, the maximum hydrate formation rate that could potentially lead to pipeline blockage and the most likely location of hydrate blockage after formation during the operation of the natural gas gathering and transportation pipeline under different influencing factors were obtained, as presented in Table 3. It can be observed that as inlet pressure and terminal pressure decrease, the maximum hydrate formation rate that could potentially lead to pipeline blockage decreases. As inlet temperature increases and terminal pressure decreases while inlet pressure decreases, the most likely location of hydrate blockage after formation shifts towards the terminal station. Under the given calculation conditions, the maximum hydrate formation rate induced by the gathering process reached  $34.96 \times 10^{-8}$  m<sup>3</sup>/h, and the farthest potential blockage location reached 2.88 km.

From the comprehensive analysis above, it is evident that during the operation of the natural gas gathering and transportation pipeline, adjustments should be made to parameters such as inlet temperature, inlet pressure, and terminal pressure. Adjusting the inlet temperature is essential to prevent the excessive formation and transportation of hydrates due to low fluid temperatures, which could lead to safety risks related to blockages. Lowering inlet pressure and terminal pressure helps mitigate threats to pipeline operational safety; however, operating the gathering system at low pressures significantly increases energy consumption, contradicting the production goal of energy conservation and reduction. Therefore, for high-pressure gathering pipelines, measures such as higher inlet temperatures, hydrate inhibitors, electric trace heating, and thermal insulation should be employed to prevent hydrate formation during the natural gas gathering process. Additionally, considering the possibility of hydrate formation during abnormal operating conditions, such as well production and network shutdowns, the use of methanol injection should still be considered to ensure production safety.

### 5. Conclusion

Addressing the risk of hydrate blockage in natural gas gathering

and transportation pipelines, this study establishes a theoretical model for the temperature field and utilizes numerical computation methods. It analyzes the influence of different inlet temperatures, inlet pressures, and terminal pressures, thereby revealing the sensitivity patterns of hydrate blockage risk during the operation of natural gas gathering and transportation pipelines.

Higher inlet temperatures lead to a reduction in the hydrate formation range, decrease hydrate supercooling, and shift the most likely hydrate blockage location towards the terminal end. Lower inlet pressures decrease the maximum hydrate formation rate, narrow the hydrate formation range, and shift the most probable blockage location towards the terminal. Lower terminal pressures reduce the maximum hydrate formation rate and shift the most likely blockage location towards the starting end. Elevated flow temperatures and reduced flow pressures contribute to ensuring the prevention and control of hydrate-related risks during the transportation process.

During the operation of natural gas gathering and transportation pipelines, appropriate adjustments to inlet temperature are necessary to prevent excessive hydrate formation and transportation caused by low fluid temperatures, thus mitigating safety risks associated with blockages. Reducing inlet pressure and terminal pressure helps mitigate threats to pipeline operational safety. However, operating the gathering system at low pressures significantly increases energy consumption, conflicting with the production goal of energy conservation and reduction. Therefore, for high-pressure gathering pipelines, measures such as higher inlet temperatures or the use of inhibitors, electric trace heating, and thermal insulation should be implemented to prevent hydrate formation during the natural gas gathering process. Additionally, considering the potential formation of hydrates during abnormal operating conditions such as well production and network shutdowns, the use of methanol injection should still be considered to ensure production safety.

#### **CRediT authorship contribution statement**

**Ao-Yang Zhang:** Writing — original draft, Writing — review & editing. **Meng Cai:** Data curation. **Na Wei:** Project administration. **Hai-Tao Li:** Data curation. **Chao Zhang:** Conceptualization, Data curation. **Jun Pei:** Formal analysis. **Xin-Wei Wang:** Project administration, Resources.

#### **Declaration of competing interest**

The authors declare no conflict of interest.

#### Acknowledgments

This research was supported by 111 Project (No. D21025), Open Fund Project of State Key Laboratory of Oil and Gas Reservoir Geology and Exploitation (Nos. PLN2021-01, PLN2021-02, PLN2021-03), High-end Foreign Expert Introduction Program (No. G2021036005L), National Key Research and Development Program (No.2021YFC2800903) and National Natural Science Foundation of China (No. U20B6005-05).

#### References

Abbasi, A., Hashim, F.M., 2022. A review on fundamental principles of a natural gas hydrate formation prediction. Petrol. Sci. Technol. 40 (19), 2382–2404. https://doi.org/10.1080/10916466.2022.2042559.

Aijaz, A., Fakhruldin, M.H., 2016. A prediction model for the natural gas hydrate formation pressure into transmission line. Petrol. Sci. Technol. 34 (9), 824–831. https://doi.org/10.1080/10916466.2016.1170842.

Akhfash, M., Aman, Z.M., Sang, Y.A., et al., 2016. Gas hydrate plug formation in

partially-dispersed water—oil systems. Chem. Eng. Sci. 140, 337-347. https://doi.org/10.1016/j.ces.2015.09.032.

- Amr, H., Amr, E., Ihab, M.E.A., 2023. Numerical sensitivity analysis of corroded pipes and burst pressure prediction using finite element modeling. Int. J. Pres. Ves. Pip. 202, 104906. https://doi.org/10.1016/j.ijpvp.2023.104906.
- Bergeron, S., Servio, P., 2009. CO<sub>2</sub> and CH<sub>4</sub> mole fraction measurements during hydrate growth in a semi-batch stirred tank reactor and its significance to kinetic modeling. Fluid Phase Equil. 276 (2), 150–155. https://doi.org/10.1016/ i.fluid.2008.10.021.
- Bykov, I.Y., Paranuk, A.A., Bunyakin, A.V., 2022. Mathematical simulation of temperature conditions of hydrate formation in the field gas collectors of the Western Pestsovaya Area of the Urengoi oil and gas condensate field. J. Eng. Phys. Thermophys. 95 (1), 223–229. https://doi.org/10.1007/s10891-022-02481-3.
- Cai, H., Zhao, L., Chen, X., et al., 2018. Optimization of temperature drop formula for annular gathering pipeline in high water cut oil region of central hebei province. Workshop 9, 2018. https://doi.org/10.4236/jpee.2018.69003.
- Chen, W., Xu, H., Kong, W., et al., 2020. Study on three-phase flow characteristics of natural gas hydrate pipeline transmission. Ocean Eng. 214, 107727. https://doi.org/10.1016/j.oceaneng.2020.107727.
- Freer, E.M., Selim, M.S., Sloan, E.D., 2001. Methane hydrate film growth kinetics. Fluid Phase Equil. 185 (1–2), 65–75. https://doi.org/10.1016/S0378-3812(01) 00457-5, 2001.
- Hammerschmidt, E.G., 1934. Formation of gas hydrates in natural gas transmission lines. Ind. Eng. Chem. 26 (8), 851–855. https://doi.org/10.1001/jie50296a010
- lines. Ind. Eng. Chem. 26 (8), 851–855. https://doi.org/10.1021/ie50296a010. Hu, J., Yang, Z., Su, H., 2023. Dynamic prediction of natural gas calorific value based on deep learning. Energies 16 (2), 799. https://doi.org/10.3390/en16020799.
- Jiang, Y., Ren, Z., Yang, X., et al., 2022. A steady-state energy flow analysis method for integrated natural gas and power systems based on topology decoupling. Appl. Energy 306, 118007. https://doi.org/10.1016/j.apenergy.2021.118007.
- Appl. Energy 306, 118007. https://doi.org/10.1016/j.apenergy.2021.118007.

  Joshi, S.V., Grasso, G.A., Lafond, P.G., et al., 2013. Experimental flowloop investigations of gas hydrate formation in high water cut systems. Chem. Eng. Sci. 97 (7), 198–209. https://doi.org/10.1016/j.ces.2013.04.019.
- Kishimoto, M., Mitarai, M., Ohmura, R., 2011. Surfactant effects on crystal growth of clathrate hydrate at interface between water and hydrophobic-guest liquid. Proc. Therm. Eng. Conf. 3—4. https://doi.org/10.1021/cg501613a.
- Kvamme, B., Kuznetsova, T., Bauman, J.M., et al., 2016. Hydrate formation during transport of natural gas containing water and impurities. J. Chem. Eng. Data 61 (2), 936–949. https://doi.org/10.1021/acs.jced.5b00787.
- Liu, W., Hu, J., Li, X., et al., 2018a. Research on evaluation method of wellbore hydrate blocking degree during deepwater gas well testing. Nat. Gas Sci. Eng. 59, 168–182. https://doi.org/10.1016/j.jngse.2018.08.027.
- Liu, W., Hu, J., Li, X., et al., 2018b. Assessment of hydrate blockage risk in long-distance natural gas transmission pipelines. J. Nat. Gas Sci. Eng. 60, 256–270. https://doi.org/10.1016/j.jngse.2018.10.022.
- Liu, W., Jin, X., Chow, T., et al., 2023. Sensitivity study of heat-pipe-ring embedded building façade for solar absorption. Energy Build. 288, 113023. https://doi.org/

- 10.1016/j.enbuild.2023.113023.
- Luo, Z., Liu, Q., Yang, F., et al., 2022. Research and application of surface throttling technology for ultra-high-pressure sour natural gas wells in Northwestern Sichuan Basin, Energies 15 (8641), 8641. https://doi.org/10.3390/en15228641.
- Misyura, S.Y., 2022. Dissociation and combustion of gas hydrates. J. Eng. Thermophys. 31 (4), 573–579. https://doi.org/10.1134/S181023282204004X.
- Parsons, S., 2023. Hydrate formation at extreme conditions. Acta Crystallogr., Sect. C: Struct. Chem. 79 (1), 1–2. https://doi.org/10.1107/S2053229622011731.
- Rao, I., Koh, C.A., Sloan, E.D., et al., 2013. Gas hydrate deposition on a cold surface in water-saturated gas systems. Ind. Eng. Chem. Res. 52 (18), 6262–6269. https:// doi.org/10.1021/ie400493a.
- Ren, G., Zhang, C., Dong, Z., et al., 2019. Hydrate deposition performance in the test string of deep water gas well. Special Oil Gas Reservoirs 26 (3), 6. https:// doi.org/10.3969/j.issn.1006-6535.2019.03.032.
- Sonne, J., Pedersen, K.S., 2009. Simulation of hydrate growth in steady state flow lines. Miner. Int. Conf. Multiphase Prod. Tech. https://onepetro.org/BHRICMPT/ proceedings-abstract/BHR09/All-BHR09/132.
- Soroush, Z., Abdollah, S., 2023. Temporal global sensitivity analysis of concrete sewer pipes under compounding corrosion and heavy traffic loads. Struct. Infrastruct. Eng. 19 (8), 1108–1121. https://doi.org/10.1080/15732479.2021.2009882.
- Sun, Z., Shi, K., Guan, D., et al., 2021. Current flow loop equipment and research in hydrate-associated flow assurance. J. Nat. Gas Sci. Eng. 96. https://doi.org/10.1016/j.jngse.2021.104276.
- Tang, Y., Yao, J., He, Y., et al., 2020. Study on pressure-controlled sliding sleeve of jet breaking for natural gas hydrate mining based on throttle pressure drop principle. Energy Sci. Eng. 8 (5), 1422–1437. https://doi.org/10.1002/ese3.616.
- Wang, J., Li, Y., Zhao, J., 2022. Simulation of the effect of hydrate adhesion properties on flow safety in solid fluidization exploitation. Petroleum. https://doi.org/ 10.1016/j.petlm.2022.04.003.
- Wang, Z., Sun, B., Wang, X., et al., 2014. Prediction of natural gas hydrate formation region in wellbore during deep-water gas well testing. J. Hydrodyn. 26 (4), 568–576. https://doi.org/10.1016/S1001-6058(14)60064-0.
- Webb, E.B., Rensing, P.J., Koh, C.A., et al., 2012. High-pressure rheology of hydrate slurries formed from water-in-oil emulsions. Energy Fuel. 26, 3504–3509. https://doi.org/10.1021/ie5008954.
- Yang, L., Shi, K., Qu, A., et al., 2023a. The locally varying thermodynamic driving force dominates the gas production efficiency from natural gas hydrate-bearing marine sediments. Energy 276, 127545. https://doi.org/10.1016/j.jenergy.2023.127545.
- Yang, Z., Liu, Z., Zhou, J., et al., 2023b. A graph neural network (GNN) method for assigning gas calorific values to natural gas pipeline networks. Energy 278, 127875. https://doi.org/10.1016/j.energy.2023.127875.
- Zhang, T., She, X., Ding, Y., 2021. A power plant for integrated waste energy recovery from liquid air energy storage and liquefied natural gas. Chin. J. Chem. Eng. 34 (6), 242–257. https://cjche.cip.com.cn/EN/10.1016/j.cjche.2021.02.008.